ORIGINAL ARTICLE

Structural and metabolic brain abnormalities in COVID-19 patients with sudden loss of smell

Maxime Niesen[1,2] · Nicola Trotta[2,3] · Antoine Noel[1] · Tim Coolen[2,4] · Georges Fayad[1] · Gil Leurkin-Sterk[2,3] · Isabelle Delpierre[4] · Sophie Henrard[2,5] · Niloufar Sadeghi[4] · Jean-Christophe Goffard[5] · Serge Goldman[2,3] · Xavier De Tiège[2,3]

Abstract

Objectives Sudden loss of smell is a very common symptom of coronavirus disease 19 (COVID-19). This study characterizes the structural and metabolic cerebral correlates of dysosmia in patients with COVID-19.

Methods Structural brain magnetic resonance imaging (MRI) and positron emission tomography with [18F]-fluorodeoxyglucose (FDG-PET) were prospectively acquired simultaneously on a hybrid PET-MR in 12 patients (2 males, 10 females, mean age: 42.6 years, age range: 23–60 years) with sudden dysosmia and positive detection of severe acute respiratory syndrome coronavirus 2 (SARS-CoV-2) on nasopharyngeal swab specimens. FDG-PET data were analyzed using a voxel-based approach and compared with that of a group of healthy subjects.

Results Bilateral blocking of the olfactory cleft was observed in six patients, while subtle olfactory bulb asymmetry was found in three patients. No MRI signal abnormality downstream of the olfactory tract was observed. Decrease or increase in glucose metabolism abnormalities was observed $(p < .001$ uncorrected, $k \geq 50$ voxels) in core olfactory and high-order neocortical areas. A modulation of regional cerebral glucose metabolism by the severity and the duration of COVID-19-related dysosmia was disclosed using correlation analyses.

Conclusions This PET-MR study suggests that sudden loss of smell in COVID-19 is not related to central involvement due to SARS-CoV-2 neuroinvasiveness. Loss of smell is associated with subtle cerebral metabolic changes in core olfactory and high-order cortical areas likely related to combined processes of deafferentation and active functional reorganization secondary to the lack of olfactory stimulation.

Keywords FDG-PET · MRI · COVID-19 · Smell loss

This article is part of the Topical Collection on Neurology

✉ Maxime Niesen
maxime.niesen@ulb.be

1. Department of Otorhinolaryngology, CUB Hôpital Erasme, Université libre de Bruxelles (ULB), Brussels, Belgium

2. Laboratoire de Cartographie fonctionnelle du Cerveau, UNI — ULB Neuroscience Institute, Université libre de Bruxelles (ULB), Brussels, Belgium

3. Department of Nuclear Medicine, CUB Hôpital Erasme, Université libre de Bruxelles (ULB), Brussels, Belgium

4. Department of Radiology, CUB Hôpital Erasme, Université libre de Bruxelles (ULB), Brussels, Belgium

5. Department of Internal Medicine, CUB Hôpital Erasme, Université libre de Bruxelles (ULB), Brussels, Belgium

Introduction

The severe acute respiratory syndrome coronavirus 2 (SARS-CoV-2) is responsible, since December 2019, of an ongoing worldwide outbreak of atypical and severe pneumonia, called coronavirus disease 2019 (COVID-19). Sudden loss of smell (i.e., anosmia) and taste (i.e., ageusia) are very common symptoms in SARS-CoV-2 infection, being reported in up to 80% of cases (for a review, see [1]).

SARS-CoV-2 infects human cells by binding to the angiotensin-converting enzyme 2 (ACE2) with contribution of the transmembrane protease serine 2 (TMPRSS2) [2]. ACE2 and TMPRSS2 appear to be widely expressed by key support (sustentacular cells, Bowman's gland, microvillar cells) and stem cells of the olfactory epithelium (OE), but not by olfactory sensory neurons (OSNs) [1]. How SARS-

CoV-2 infection of OE cells leads to sudden smell loss remains hypothetical. The causal link might involve (i) blockage of the olfactory cleft due to focal OE inflammation, (ii) alteration of OSNs function, or (iii) widespread damage to OE and subsequently OSNs with variable time to recovery depending on the extent of stem cell damage [1]. Changes in olfactory bulbs (OB) and variable cortical (e.g., orbitofrontal cortex) or subcortical (e.g., thalamus, hypothalamus, brainstem) areas have also been disclosed by magnetic resonance imaging (MRI) [3–7] or positron emission tomography (PET) [8, 9] in some COVID-19 patients with or without anosmia. Whether these central nervous system (CNS) abnormalities are indicative of potential SARS-CoV-2 neuroinvasion triggering or triggered by anosmia is still a matter of debate [1].

To get novel insights into the possible CNS involvement in COVID-19 patients with sudden dysosmia, we used a hybrid PET and MRI system (PET-MR) to investigate the brain structure and regional glucose metabolism of SARS-CoV-2-infected patients with sudden loss of smell. We specifically searched for MRI signal and metabolic abnormalities along the olfactory system and brain areas previously shown to be involved in the pathophysiology of non-COVID-19-related anosmia. We also searched for any sign of acute brain abnormalities.

Methods

Study design and participants

From April 3, 2020 to May 18, 2020, dysosmic patients in the context of a SARS-Cov-2 infection were prospectively recruited at the CUB Hôpital Erasme based on the following criteria: (i) sudden loss of smell; (ii) positive SARS-CoV-2 detection (direct antigen detection or reverse transcriptase polymerase chain reaction) on nasopharyngeal swab specimen; (iii) no prior history of neurological, psychiatric, nasal, sinus, or olfactory disorders; (iv) MRI compatibility; and (v) formal acceptance to participate to the study.

Objective evaluation of olfactory dysfunction was performed using the "*identification test*" included in the Sniffin Sticks Battery (Burghart Messtechnik, Wedel, Germany) at the time of PET-MR data acquisition. The evolution of dysosmia was assessed at the time of manuscript submission using qualitative anamnesis and visual analog scale (0, no smell at all; 10, normal olfactory function). No olfactory training or objective evaluation using the identification test was performed at follow-up. Clinical data were retrieved from patients' anamnesis and medical records.

For PET data analyses, a PET-MR data set acquired in the context of other neuroimaging studies and composed of 26 healthy subjects (5 females, 21 males, mean age: 35 years,

age range: 22–52 years) without any history of COVID-19, smell or taste disorders was used as control group.

Standard protocol approvals, registrations, and patient consents

Studies were carried out at the CUB Hôpital Erasme (Brussels, Belgium). Participants contributed to the corresponding studies approved by the institutional Ethics Committee after written informed consent (References: P2020/204, CCB: B4062020000031; P2017/541, CCB: B406201734197).

PET-MR data acquisition

Cerebral PET and MRI data were obtained using a 3 T hybrid PET-MR scanner (SIGNA™, GE Healthcare, Chicago, IL) in accordance with COVID-19 institutional hygienic and safety rules.

MRI sequences have been described in details elsewhere [5]. They consisted in whole-brain axial 3D T1-weighted imaging (WI), axial T2WI, sagittal 3D T2WI fluid-attenuated inversion recovery (FLAIR), axial 3D susceptibility-WI (SWI), axial diffusion-WI (DWI), and a coronal T2WI centered on olfactory bulbs.

For PET data acquisitions, participants fasted for at least 4h were awake in an eye-closed rest and received an intravenous bolus injection of 3–5 mCi (111–185 MBq) of $[^{18}F]$-fluorodeoxyglucose (FDG) before PET-MR data acquisition. Forty minutes post-injection, a 20-min data acquisition was performed. PET data were reconstructed using the fully 3D iterative reconstruction algorithm VUE Point FX-S, which takes into account the time-of-flight (TOF) information and the correction for the point spread function (PSF) of the system. The algorithm was configured with 10 iterations, 28 subsets, and a standard Z-axis filter cut-off at 4 mm. The photons' attenuation was corrected with a MRI-based map (MRAC) acquired simultaneously. PET images were displayed in a $256 \times 256 \times 89$ matrix format, with a slice thickness of 2.78 mm. The reconstructed files were downloaded in their original format (DICOM, ECAT, Interfile) for meta-information and converted in NIfTI format for subsequent analysis.

MRI data analysis

MRI data were reviewed by two experienced neuroradiologists (T.C. and I.D.) following a systematic and comprehensive visual assessment procedure previously described [5]. Brain MRI findings were divided into recent (i.e., potentially related to SARS-CoV-2) and long-standing (i.e., unlikely related to SARS-CoV-2) changes [5]. The Lund-Mackay score for chronic rhinosinusitis [10] was used for the visual

assessment of incidental paranasal sinus inflammation and adapted to evaluate olfactory cleft obliteration (0: normal; 1: partial obliteration; 2: total obliteration) at the level of the OB. Final reports were then discussed with neurologists (S.G., X.D.T.), neuroradiologist (N.S.), otorhinolaryngologists (M.N., A.N., G.F.), and internists (S.H., J-C.G.)

PET data analysis

FDG-PET data were analyzed using the voxel-based Statistical Parametric Mapping software (SPM8, http://www.fil.ion.ucl.ac.uk/spm/, Wellcome Trust Centre for Neuroimaging, London, UK) based on conventional subtractive and correlation analyses previously used by our group and described in details elsewhere [11–15].

Briefly, PET images were spatially normalized into the Montreal Neurologic Institute template (MNI, Montreal Neurologic Institute, Quebec, Canada) and then smoothed using a 12-mm full-width at half-maximum Gaussian isotropic kernel. Global activity normalization was performed by proportional scaling.

For individual- and group-level subtractive analyses, we constructed general linear models (GLMs) of the preprocessed FDG-PET data of dysosmic patients—taken individually or as a group—and healthy subjects taken as separate groups. Separate t-contrasts identified brain areas where glucose metabolism was significantly lower or higher in dysosmic patient(s) compared with healthy subjects.

For correlation analyses, we constructed GLMs of the preprocessed FDG-PET data of dysosmic patients taken as one group. Scores of the *identification test* (Sniffin Sticks Battery) and duration (days) of smell loss were introduced as covariates of interest centered around condition means in separate GLMs. Separate t-contrasts identified brain regions showing significant positive or negative correlations between the covariates of interest and regional cerebral glucose metabolism. For significant voxels, regression plots and associated slope coefficients/p values (Pearson's correlation) between glucose metabolism and covariates of interest were obtained in Matlab R2017a (MathWorks Inc.).

Participant's age was introduced as covariate of no-interest in all GLMs to avoid potential aging confounds. Gender was not used as covariate of no-interest considering the unbalanced gender profile between dysosmic patients and healthy subjects.

Results were considered significant at $p < .05$ corrected for multiple comparisons over the entire brain volume (family wise error, FWE). As the FWE rate may be considered as too conservative at the individual level or for group-level analyses based on small samples sizes, results were also deemed significant at $p < .001$ uncorrected (cluster size $k \geq 50$ voxels) to minimize type II errors. This more liberal threshold was adopted only when voxels involved brain areas previously reported as (i) involved in the processing of odors in healthy subjects [16–19] or as (ii) metabolically abnormal in COVID-19-related or non-COVID-19-related anosmia [8, 9, 20–22]. Since several of those studies did not report the [x, y, z] coordinates of their significant effects in the Montreal Neurological Institute (MNI) space, we could not properly apply small volume correction to our data.

Finally, because we were using a high-resolution digital PET-MR system, we checked if the level of OB glucose metabolism in COVID-19 patients and healthy subjects could be evaluated, in order to gain further insights into the pathophysiology of COVID-19-related dysosmia. Unfortunately, it appeared that the level of OB glucose consumption was too weak to perform any analysis.

Results

Patients' clinical characteristics

Table 1 describes the patients' clinical characteristics.

Fourteen patients (11 females, 3 males, mean age: 43 years, age range: 23–60 years) fulfilled the inclusion criteria. Two patients were excluded from further analyses due to magnetic artifacts covering the nasal cavity and orbitofrontal cortex (1 patient) and to the presence of a large right sylvian arachnoid cyst that would interfere with the normalization procedure (1 patient). Therefore, the final sample considered for the study was composed of 12 patients.

In those patients, subjective loss of smell occurred on average 15 days (± 9 days) before PET-MR data acquisition. It was the predominant symptom related to SARS-CoV-2 infection in seven patients. Other symptoms were dyspnea (five patients), asthenia (five patients), and gastro-intestinal symptoms (three patients). Six patients also presented with headaches. One patient was hospitalized for the management of COVID-19 respiratory symptoms, while the others were outpatients.

Olfactory disorder was confirmed in each of the 12 SARS-CoV-2-positive patients by objective olfactory testing. The mean *identification test* score was 8/16 (± 1.4) and documented hyposmia in 5 patients (scores between 9 and 11) and anosmia in 7 patients (scores ≤ 8).

Positive evolution of dysosmia was observed in all patients. Five patients fully or almost fully recovered (4 to 10 weeks after onset; visual analog scale: 9 or 10). Seven patients still complained of relative hyposmia (improvement observed from 1 to 16 weeks after onset; visual analog scale: 6 to 8).

Structural MRI abnormalities

Table 2 and Fig. 1 describe the MRI findings observed in dysosmic patients.

Table 1   Clinical characteristics of the patients

Clinical characteristic	% of Patients ($n_{tot} = 12$)
Mean age (range), years	42.6 (23 – 60)
Mean Body Mass Index (range), kg/m^2	24.8 (22 – 29.8)
Female gender	83.3 (10)
Active smoker	8.3 (1)
Hospitalisation	8.3 (1)
SARS-CoV-2 detection	
Direct antigen detection	25 (3)
Reverse transcriptase PCR	75 (9)
Comorbidities	
Respiratory allergy	50 (6)
Asthma	8.3 (1)
Hypertension	16.7 (2)
Hypothyroidism	8.3 (1)
Diabetes	0
Symptoms	
Dysosmia	100 (12)
Dysgueusia	91.7 (11)
Myalgia, Arthralgia	75 (10)
Cough	66.7 (8)
Rhinorrhea	66.7 (8)
Fever	50 (6)
Headache	50 (6)
Dyspnea	41.7 (5)
Asthenia	41.7 (5)
Diarrhea	25 (3)
Nausea, Vomiting	16.7 (2)
Rash	8.3 (1)
Throat pain	8.3 (1)
Objective olfactory assessment	
Anosmia	58.3 (7)
Hyposmia	41.7 (5)

Subtle OB asymmetry was found in three patients with no associated bulbar signal abnormality. Four patients had no olfactory cleft obliteration, two had partial obliteration of one olfactory cleft, and six patients had bilateral olfactory cleft obliteration (bilateral and complete in four). Discrete signs of sinus inflammation were found in six patients (Lund-Mackay score less than 6). No sign of recent brain abnormality was found in any of the patients. Non-systematic long-standing brain MRI findings (e.g., periventricular halo, small arterial aneurysm, developmental venous anomaly, focal microbleed) were found in all but one patient. Of note, we did not find any significant correlation between the *identification test* score and the Lund-Mackay score of the olfactory cleft (Pearson correlation, $r = -0.178$, $p = .58$) nor with the Lund-Mackay score of the paranasal sinuses (Pearson correlation, $r = 0.276$, $p = .39$).

Regional cerebral glucose abnormalities

Tables 3 and 4 and Figs. 2, 3, 4 describe the regional cerebral glucose abnormalities observed at the individual (Fig. 2) and group (Fig. 3) levels in dysosmic patients, as well as the results of correlation analyses (Fig. 4).

None of the results of subtractive (individual and group levels) and correlation (identification test scores and dysosmia duration) analyses were significant at the FWE rate (i.e., after correction for multiple comparisons over the entire brain volume). Still, some results were considered significant at a more liberal statistical threshold (i.e., $p < .001$ uncorrected, cluster

size $k \geq 50$ voxels) in brain areas previously found to be involved in odor processing or in the pathophysiology of anosmia.

At this less stringent statistical threshold, all patients showed significant decrease (3 patients) or increase (1 patient) in regional cerebral glucose metabolism, or a combination of both (8 patients) at the individual level. Hypometabolic areas involved nodes of the core olfactory network (4 patients), somatosensory (1 patient) or visual (1 patient) cortical areas, the cerebellum (2 patients), or higher-order neocortical areas (9 patients) mainly encompassing the attentional, emotional, or default mode (DMN) networks. Hypermetabolic areas also involved nodes of the core olfactory network (6 patients), the cerebellum (1 patient), or high-order neocortical areas (5 patients) belonging to the attentional network or the DMN.

At the group level, compared with healthy controls, dysosmic patients presented significant decrease in regional glucose consumption in bilateral dorso-lateral prefrontal cortex (DLPFC), bilateral frontal eye fields (FEF), and in the right anterior cingulate cortex (ACC). Significant ($p < .001$ uncorrected) hypermetabolic areas were also found in the left orbitofrontal cortex, the right posterior parietal cortex (PCC), and in the right thalamus.

Significant negative correlation was found between the *Identification test* score and cerebral glucose metabolism in the right FEF, the left orbitofrontal cortex, and in the left PCC, indicating that a more severe deficit was related to a higher glucose metabolism in these brain regions.

Significant positive correlation was found between the duration of dysosmia and brain metabolism in bilateral orbitofrontal cortex and in the right DLPFC, MPFC, and PPC, indicating that a longer duration of loss of smell was related to a higher glucose metabolism in these brain regions.

Of note, no significant correlation was found between the *Identification test* score and the duration of dysosmia (Pearson correlation, $r = 0.07$, $p = .82$).

Discussion

This PET-MR study performed in 12 patients with sudden loss of smell due to SARS-CoV-2 infection demonstrates (i) bilateral obliteration of the olfactory cleft in 50% of the patients, (ii) subtle OB asymmetry in 25% of the patients, (iii) the absence of MRI signal abnormality downstream of the olfactory tract in all patients, (iv) subtle regional glucose metabolism changes mainly in nodes of olfactory and high-order brain networks, and (v) modulation of regional cerebral glucose metabolism by the intensity and the duration of SARS-CoV-2-related loss of smell.

Included patients were mainly young adults (mean age: 42.6 years) with a very low frequency of comorbidities (e.g.,

Table 2 Structural MRI findings

Patient	Age	Gender	IT score	Asymmetry of olfactory bulbs	Olfactory clefts*		Paranasal sinuses*							
					Right	Left	Right				Left			
							F	E	S	M	F	E	S	M
1	51	H	9	-	0	0	0	0	0	0	0	0	0	0
2	23	F	6	-	0	0	0	0	0	0	0	0	0	0
3	35	F	10	-	0	0	0	1	1	1	0	1	0	1
4	44	H	9	-	1	2	0	0	0	0	0	0	0	0
5	56	F	5	-	2	2	0	1	0	0	0	0	0	0
6	60	F	8	-	1	2	0	0	0	0	0	0	0	0
7	54	F	8	Left > right	2	2	0	0	0	0	0	0	0	
8	41	F	7	-	2	2	1	1	1	1	0	1	0	1
9	30	F	7	Left > right	0	1	0	0	0	0	0	1	0	0
10	47	F	8	Left > right	0	0	0	0	0	0	0	0	0	0
11	28	F	8	-	2	2	0	0	0	0	0	0	0	0
12	43	F	9	-	1	0	0	0	0	0	0	0	0	0

IT identification test, F frontal, E ethmoidal, S sphenoid, M maxillary;

*Lund-MacKay Score: 0 = no sign of inflammation (tolerance for small cysts or visible mucosal lining < 1 mm), 1 = signs of inflammation or partial obliteration, 2 = total obliteration

hypertension, diabetes) usually associated with severe forms of COVID-19. Their main symptoms were altered sense of smell and taste; the latter being reported by all but one patient. Objective assessment of taste was not available. Considering the recognized ambiguity between taste and smell perception [23, 24], we preferred not relying on subjective assessment of taste and we concentrated the objective clinical assessment on the smell deficit. About 50–67% of the patients also had clinical signs of cold with cough, rhinorrhea, or fever. Only one patient was hospitalized in a non-intensive COVID-19 ward for the management of his respiratory distress while all the other were outpatients. Overall, the clinical characteristics of our patients' population are in line with those of SARS-CoV-2-positive patients with loss of smell and taste as predominant symptoms [25–28]. This rather small group of patients therefore appears as representative of COVID-19 dysosmic patients. Their clinical characteristics contrast (in terms of age, comorbidities, clinical presentation) with those of patients with severe forms of COVID-19 who died in the same institution (i.e., CUB Hôpital Erasme) during the same period [5].

The evolution of dysosmia was favorable in all patients but 58% of them still complained of incomplete recovery more than 15 weeks after the onset of symptoms. Long-lasting

Fig. 1 Axial T2-weighted coronal images demonstrating bilateral and complete obliteration of the olfactory clefts (white single arrows) with (**a**) no associated olfactory bulb asymmetry and with (**b**) asymmetry of the olfactory bulbs (left (L) bulb relatively enlarged, white double arrow). The criblate plate is illustrated by the dotted line
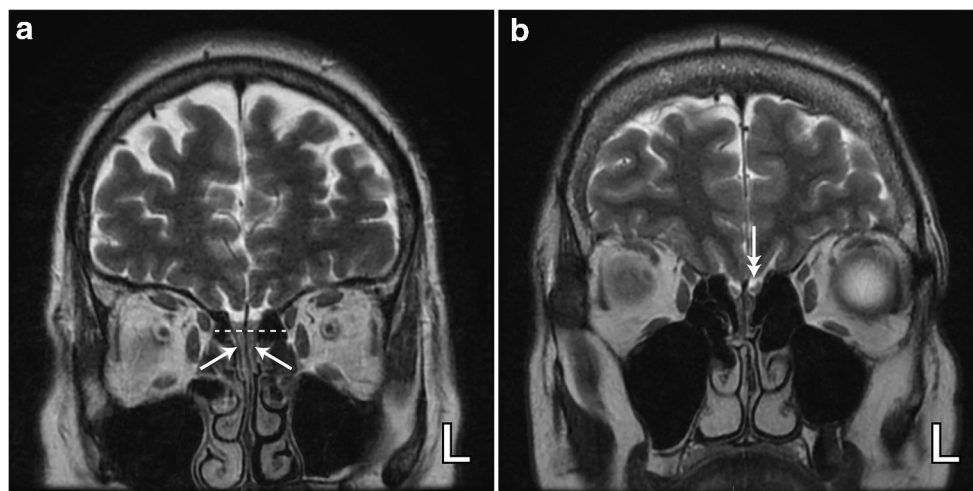
Table 3 MNI coordinates, cluster size (*k*), and *t* value (*T*) of cortical areas with significant hypo- and hypermetabolism (a) at the group level and (b) at the individual level

Hypometabolism

#	Region	x	y	z	Cluster-size	T-score
a. Group-level						
	FEF	−32	−14	62	113	4.51
		36	−8	56	77	4.13
	DLPFC	48	4	30	209	4.37
		−22	10	58	87	4.06
	Anterior cingular cortex	6	22	24	142	3.78
b. Individual-level						
1	FEF	44	48	12	1606	5.78
		−26	56	12	340	5.66
		26	22	58	80	4.63
		−26	14	60	70	4.19
	Posterior parietal cortex	−48	−66	30	140	4.89
		−40	−66	50	153	4.81
		36	−42	70	127	4.16
	Anterior cingular cortex	−2	34	32	1305	5.04
	MPFC	−4	26	58	143	4.81
	DLPFC	−50	22	24	78	3.93
2	Posterior parietal cortex	34	−48	68	60	3.91
		−34	−42	64	50	3.84
3	Piriform cortex	16	26	−30	207	5.96
	Hippocampus	−24	−16	−20	90	4.08
4	SMC	−10	4	72	68	5.35
	DLPFC	−44	10	32	74	4.64
5	Post-central gyrus	−22	−28	72	73	4.83
	Posterior parietal cortex	20	−72	58	82	4.80
		−44	−22	56	60	4.35
	Insula	−46	12	−4	91	4.57
	VLPFC	58	10	28	74	4.29
6	FEF	−28	14	58	386	6.39
	VLPFC	58	20	30	110	5.20
	Posterior parietal cortex	36	−52	66	68	4.58
		−46	−52	56	63	4.41
	Superior frontal gyrus	10	12	66	177	4.13
	Inferior parietal lobule	−60	−22	42	20	3.77
7	n.s.					
8	Middle temporal gyrus	−60	−36	−2	84	4.92
	Orbitofrontal cortex	−38	20	−12	420	4.53
	Piriform cortex	30	24	−22	67	4.28
9	Insula	−32	−16	12	311	5.61
	Cuneus	14	−74	34	357	4.99
	Occipital cortex	−34	−86	14	93	4.49
	Vermis	0	−48	−38	106	4.14
	Hippocampus	−26	−18	−20	58	4.09
	Middle temporal gyrus	−60	−4	−20	116	4.07
	Orbitofrontal cortex	−2	16	−18	70	4.04
	Lingual gyrus	8	−88	−6	220	3.93
		10	−60	−2	73	3.39
10	Middle temporal gyrus	−62	−4	−18	345	4.96
	Cerebellum	−40	−44	38	103	4.44
	Posterior cingular cortex	−6	−52	14	80	4.09
11	DLPFC	44	6	28	58	4.80
12	Thalamus	14	−22	14	263	5.03

Hypermetabolism

#	Region	x	y	z	Cluster-size	T-score
a. Group-level						
	Orbitofrontal cortex	−30	38	0	52	4.36
	Posterior parietal cortex	24	−42	82	55	4.23
	Thalamus	24	−18	8	89	4.05
b. Individual-level						
1	Cerebellum	30	−42	−46	1811	6.13
		−10	−44	−50	118	4.06
	Thalamus	26	−26	6	398	4.56
2	n.s.					
3	n.s.					
4	Anterior temporal pole	40	4	−38	97	3.83
5	Anterior temporal pole	32	14	−36	119	4.67
6	Orbitofrontal cortex	−38	28	−26	142	4.85
	Piriform cortex	30	22	−30	89	4.44
	Anterior temporal pole	−48	2	−16	52	4.16
	Hippocampus	24	8	−16	61	4.07
7	DLPFC	−38	48	30	56	4.75
8	n.s.					
9	Precuneus	14	−58	42	152	5.21
	Precuneus	−10	−60	42	135	4.79
	Posterior parietal cortex	−50	−66	38	53	4.17
10	DLPFC	−42	52	4	137	4.59
	Posterior parietal cortex	−42	−68	32	112	4.52
11	FEF	−32	10	44	152	5.35
		34	16	36	117	4.60
	Posterior parietal cortex	28	−44	52	156	4.46
12	Precuneus	8	−58	48	435	6.06
	Orbitofrontal cortex	26	44	−14	102	4.44
		−32	40	−14	155	4.06
	SMC	16	−26	56	99	4.28

dysosmia in these patients could be the secondary consequence of the death of OE support and stem cells; the latter playing a crucial role in regenerating OE [1].

Structural MRI abnormalities

Bilateral (partial or complete) obliteration of the olfactory cleft was observed in about half of dysosmic patients. Other patients had either unilateral partial obliteration (three patients) or no MRI sign of olfactory cleft inflammation (four patients, one with signs of sinusitis). These findings are in line with imaging studies of the nasal cavity in COVID-19 patients with sudden loss of smell that either showed normal (see, e.g., [26, 27, 29]) or focal inflammation of the OE with obliteration of the olfactory cleft (see, e.g., [26, 30]). This demonstrates that obliteration of the olfactory cleft due to focal OE inflammation is not the only possible pathophysiological mechanism underlying SARS-CoV-2-related dysosmia [1].

Three dysosmic patients showed subtle OB asymmetry, with no OB MRI signal abnormality. One had complete and bilateral obliteration of the olfactory cleft, while the two others had either partial unilateral obliteration or no sign of OE inflammation at all. Previous MRI studies have demonstrated MRI changes in OB in patients with SARS-CoV-2-related

anosmia [3, 4, 26] or in non-survivors of severe COVID-19 [5], suggesting some degree of central involvement at the origin of dysosmia in a subset of patients [1]. Results of the present study show that SARS-CoV-2-related OB involvement is not the main mechanism at the basis of acute loss of smell in COVID-19. Whether these OB abnormalities are associated with direct infection of OSNs or mitral cells remains doubtful considering the absence of ACE2 expression demonstrated in these cells [1]. Infection of vascular pericytes in the OB—in which there is evidence of ACE2 expression—might actually be responsible for OB MRI signal abnormalities found in some dysosmic patients. This hypothesis would be consistent with clinical evidence showing that SARS-CoV-2 predominantly influences the brain indirectly through effects on brain vasculature [1].

No acute MRI signal abnormality was found downstream of the olfactory tract (or the rest of the brain), which is in line with most previous MRI studies performed in anosmic or severe forms of COVID-19 (see, e.g., [3, 5]). Still, rare cases of possible SARS-CoV-2-related limbic encephalitis have been reported in the literature (see, e.g., [31–33]), suggesting that SARS-CoV-2 might potentially reach the brain via, e.g., the olfactory nerves, like other neurotropic viruses such as herpes simplex virus [34, 35]. Still, the question remains open

since limbic encephalitis might be para-infectious (i.e., without local viral involvement) and the neuroinvasive capacity of SARS-CoV-2 to directly infect neurons remains, to the best of our knowledge, yet unproven [1]. MRI data from the present study do not support the involvement of central olfactory pathways in SARS-CoV-2-related sudden loss of smell.

Of note, a COVID-19 patient has been reported with FLAIR hyperintensities bilaterally in the OB and in the right gyrus rectus/orbitofrontal cortex 4 days after the onset of SARS-CoV-2-related anosmia [3]. In that case, FLAIR abnormalities resolved 28 days later on a subsequent MRI [3]. Based on this single-case report, it might be speculated that OB and brain MRI abnormalities are only present at the very early phase of sudden loss of smell [3]. In this study, all PET-MR investigations were performed during the patients' symptomatic phase, with 60% of them done > 10 days after the onset of dysosmia. We cannot therefore exclude that some of our negative MRI findings are due to the rather late nasal and brain imaging. Further longitudinal studies are needed to better characterize the chronology of MRI abnormalities in this condition.

Regional brain glucose metabolism abnormalities

At the individual level, decreases or increases in regional cerebral glucose metabolism commonly involved the core olfactory network or other brain areas belonging to other sensory or high-level cognitive networks, as well as the cerebellum. These diversified findings translated at the group-level into subtle ($p < .001$ uncorrected) regional decreases and increases in glucose consumption that, unexpectedly, did not involve

nodes of the core olfactory network per se (apart from the thalamus), but rather high-order neocortical areas. Although surprising at first glance, these individual- and group-level results are in line with (i) results of fMRI studies performed in healthy subjects showing that odor processing not only recruits the core olfactory network but also other brain structures such as high-order neocortical areas (for reviews, see, e.g., [16, 36]), (ii) results of structural MRI investigations showing that dysosmic patients from various causes present changes in gray matter volume in numerous high-order neocortical areas similar to those observed in our population (see [37] for a review), and (iii) results of functional neuroimaging investigations done in dysosmic patients during olfactory stimulation, showing significant changes in the activity of similar high-order neocortical areas compared with healthy subjects [20, 37–39]. Functional neuroimaging studies performed in humans have demonstrated that, while smelling single odors activates the core olfactory network, higher-level olfactory tasks (i.e., discrimination of odor quality, odor recognition memory, or odor familiarity judgment) recruit brain areas outside the core olfactory network, including the cerebellum, cortices involved in other sensory modalities such as somatosensory or visual functions, and brain areas involved in high-order functions (for reviews, see [16, 36, 40]). The more complex the olfactory task is, the more remote these high-order areas are in terms of connection with the core olfactory network [16]. These long-range connections explain part of the olfactory experience, i.e., odors can immediately elicit strong emotions, memories, and mental images [16]. In light of this body of evidence, our results lead us to the hypothesis that SARS-CoV-2-related sudden loss of smell

Table 4 MNI coordinates, cluster size (k), Pearson's correlation coefficient (r), and T-score of cortical areas with significant correlation between the olfactory function (assessed by the Identification Test score) and cerebral glucose metabolism and between the duration of smell loss and brain metabolism

Covariate of interest	Region	Mini coordinates			Cluster size	Pearson's r	T-score
		x	y	z			
Olfactory function	FEF	30	6	48	87	− 0.97	12.60
	Posterior parietal cortex	− 22	− 54	46	60	− 0.94	8.20
	Orbitofrontal cortex	− 12	68	0	88	− 0.92	7.07
		− 38	54	− 10	61	− 0.92	6.68
Duration of anosmia	MPFC	0	48	46	113	0.96	10.25
		6	32	62	68	0.93	8.08
	DLPFC	38	32	34	143	0.94	8.73
		48	24	18	87	0.90	6.32
	Orbitofrontal cortex	− 28	66	0	50	0.91	6.57
		34	32	− 10	66	0.90	6.44
		− 36	34	− 14	198	0.89	5.97
	Posterior parietal cortex	24	− 66	54	73	0.90	6.25

*DLPFC* dorso-lateral prefrontal cortex, *FEF* frontal eye fields, *MPFC* medial prefrontal cortex
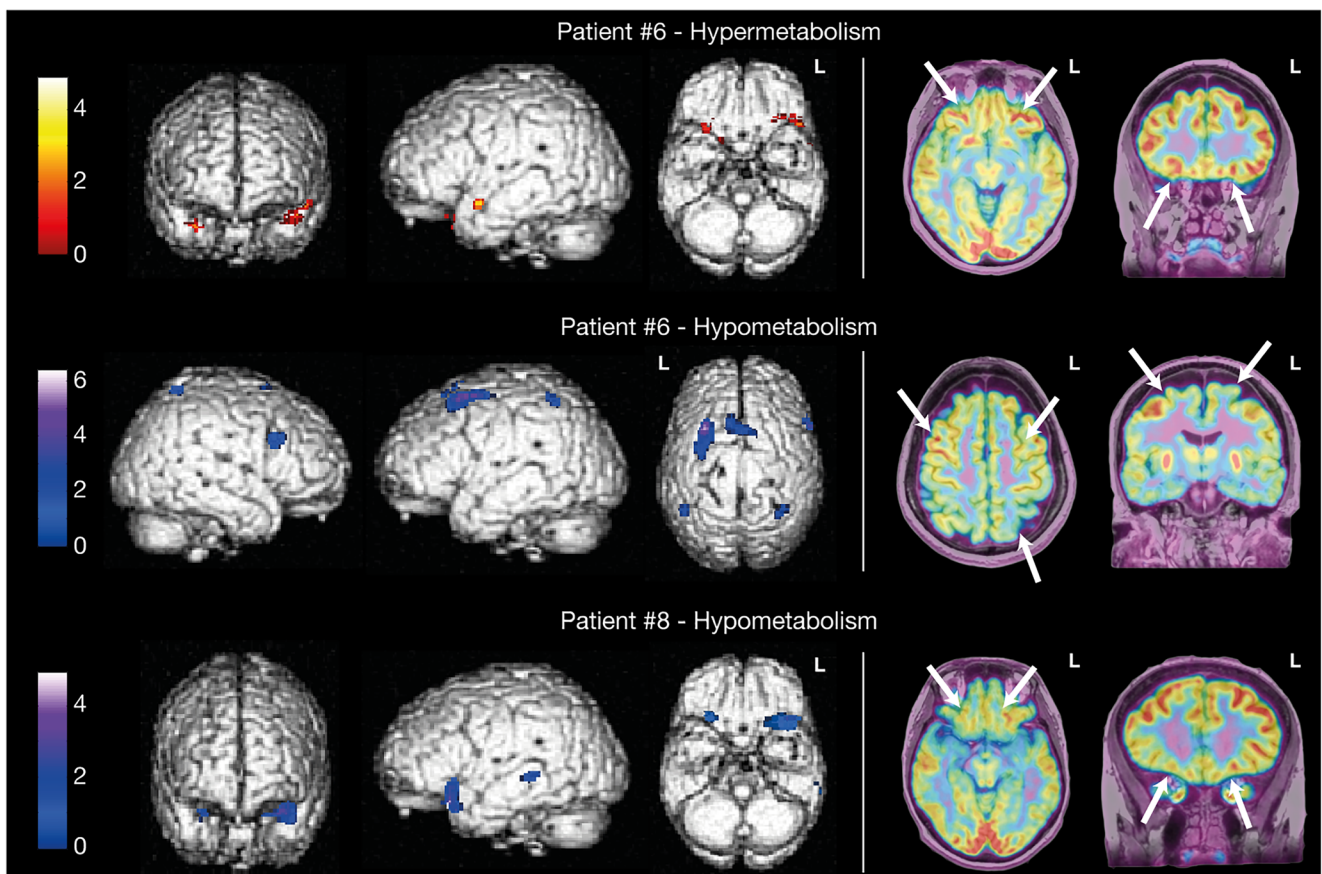
Fig. 2 Left: regional hyper- (red to white color scale) and hypo- (blue to white color scale) metabolism in two typical patients rendered on a 3D canonical brain. Images are thresholded at $p < .001$ uncorrected ($k \geq 50$ voxels). Right: native FDG-PET images co-registered on the patients' 3D T1 MRI sequence. White arrows point towards the brain areas showing significant metabolic changes at the uncorrected statistical threshold illustrated on the left part of the figure

induces changes in glucose consumption in core olfactory and other brain areas due to alterations in both basic and higher olfactory functions.

Critically, correlation analyses between regional cerebral glucose metabolism and the severity/duration of SARS-CoV-2-related smell loss brought additional insights into the
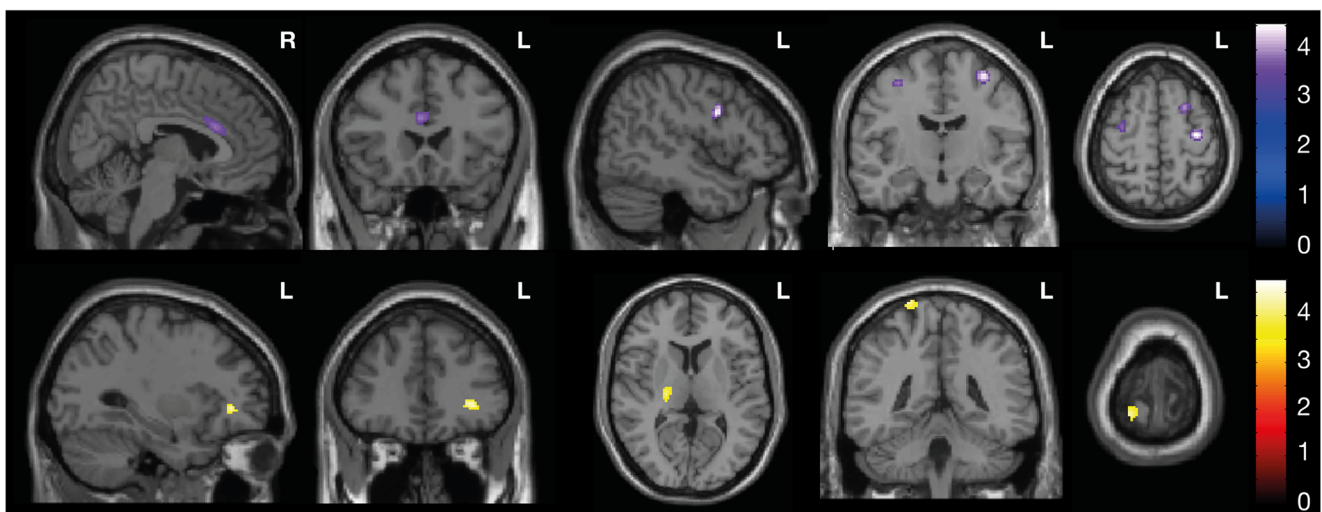
Fig. 3 Regional cerebral glucose metabolic abnormalities observed at the group level. Legend: regional hypometabolism (top) and hypermetabolism (bottom) observed at the group level. Images are thresholded at $p < .001$ uncorrected ($k \geq 50$ voxels)

origin of the metabolic changes observed at the individual level. They indeed revealed a modulation of brain glucose consumption by the severity (negative correlation with the score on the "*identification test*") and the duration (positive correlation) of dysosmia. Intriguingly, severe loss of smell (as documented by a low score on the "*identification test*") was associated with a higher glucose metabolism in some olfactory core (e.g., orbitofrontal cortex) and high-order brain areas (FEF and PCC), while patients with more preserved olfactory function had lower glucose metabolism in these brain areas. Although these results appear rather counterintuitive, they are in line with those of a previous FDG-PET study, which also showed a negative correlation of regional glucose consumption with the level of loss of smell [21]. By contrast, longer duration of loss of smell was associated with a higher glucose metabolism in some core (e.g., orbitofrontal cortex) and high-order brain areas (DLPFC, MPFC, PCC). Importantly, no correlation was found between the intensity and the duration of smell loss. These correlation data actually shed light on the mixed individual-level FDG-PET findings that translate into rather subtle group-level findings. The regional decrease in metabolism, essentially observed in patients with moderate smell loss, is probably attributable to a deafferentation phenomenon as observed, e.g., in sudden visual loss due to non-infectious disorders [41, 42]. By contrast, the increased or preserved metabolism, essentially associated with either severe or long-lasting loss of smell, could be related to functional reorganization/plasticity mechanisms. Such mechanisms involve, in particular, compensatory processes, unmasking of already existing but inactive neural connections, or the avoidance of maladaptive neural processes [43]. The hyperactivity of some brain areas may also relate to some forms of olfactory mental imaging associated with spontaneous repetitive odor search [44], or to emotional/behavioral consequences of severe or prolonged anosmia [45].

Considering that metabolic abnormalities were not associated with any MRI signal abnormality, they probably do not represent neuroimaging evidence supporting the neuroinvasive potential of the SARS-CoV-2 but rather functional cerebral markers of the olfactory deficit. Furthermore, as the observed abnormalities were akin to the structural and functional neuroimaging abnormalities previously reported in patients with dysosmia of other aetiologies (e.g., idiopathic, post-viral, traumatic) [20, 21, 37–39], they are probably not specific of COVID-19. A comparison with a group of patients with non-COVID-19-related dysosmia would be required to determine if some of the findings in COVID-19 are specific of this condition.

Limitations of the study

PET-MR data were acquired in a small group of patients at different moments after the onset of dysosmia with no longitudinal neuroimaging follow-up. Although this approach proved its value in correlation analyses with regional cerebral metabolism, it did not allow proper characterization of the chronology of structural and metabolic abnormalities in COVID-19-related dysosmia. Also, the rather limited number of patients included in this study may have impacted the statistical power of group-level subtractive and correlation FDG-PET analyses. The consequent reliance on a more liberal statistical threshold than the FWE rate (i.e., $p < .001$ uncorrected, cluster size $k \geq 50$ voxels) may have caused false-positive results. The risk of such type 1 error was, however, limited by only considering significant at these uncorrected threshold, findings in brain areas previously found to be involved in odor processing or in the pathophysiology of anosmia. They were also in accordance with the visual analysis of native FDG-PET data. Further studies in larger populations of patients are therefore mandatory to confirm the robustness of our neurometabolic findings.

This study did not include any objective evaluation of taste function as it was not available at our center at the start of the COVID-19 pandemic and was very difficult to obtain during this sanitary crisis. Considering that all but one patient complained about altered sense of taste, it would have been of great interest to investigate the brain metabolic changes specifically associated with dysgeusia. As discussed above, due to the recognized ambiguity between taste and smell perception [23, 24], we decided not to include any correlation analyses with the subjective evaluation of taste (i.e., visual analog scale).

For voxel-based FDG-PET data analyses, we relied on a group of healthy subjects who had undergone PET-MR imaging in the context of an unrelated neuroimaging study. This was due to the difficulty to perform neuroimaging research investigations in healthy subjects in an academic hospital environment during the ongoing COVID-19 pandemics. For that reason, healthy subjects did not undergo any objective or subjective evaluation of smell and taste at the time of the PET-MR data acquisition. Also, the group of healthy subjects was not properly matched for age and sex with the included COVID-19 patients. Therefore, age was introduced as a covariate of non-interest in voxel-based FDG-PET data analyses, which limits the potential confound associated with this variable in our results. A similar approach could not be applied to accommodate the gender unbalance between patients and control groups, but the findings do not match reported gender differences in cerebral glucose metabolism [46–48], while being in line with results of previous FDG-PET studies on dysosmia [9, 20, 21]. Finally, the ongoing COVID-19 pandemics in Belgium also impeded the possibility to investigate patients with non-COVID-19-related dysosmia or to organize olfactive stimulation during functional neuroimaging in groups of dysosmic patients and matched healthy subjects, the latter also requiring a specific expertise not available at
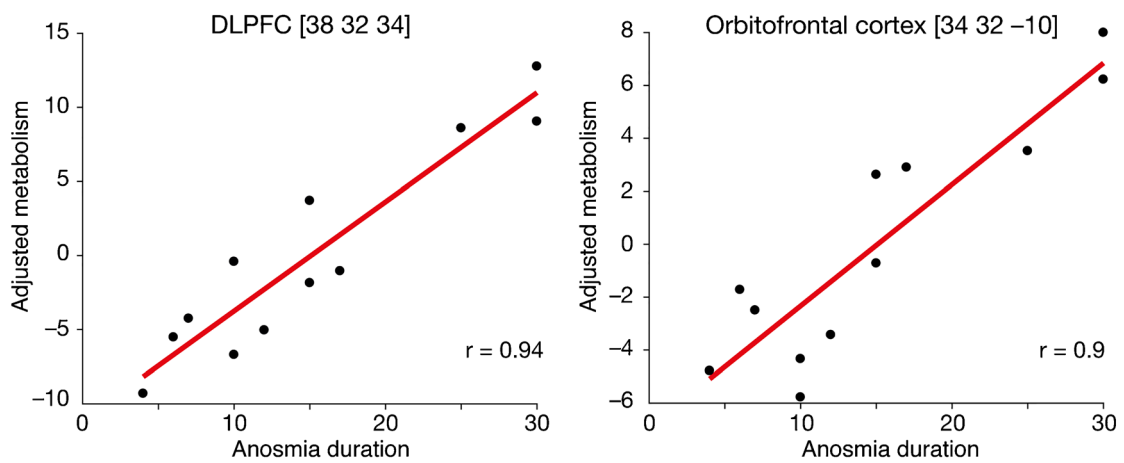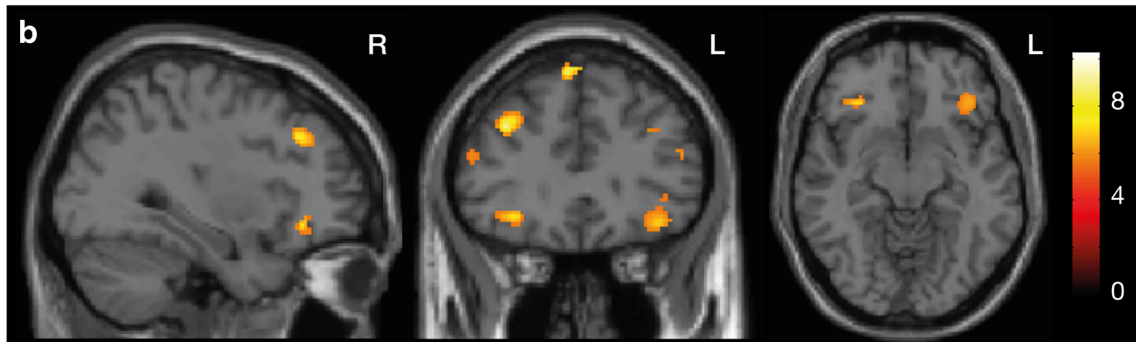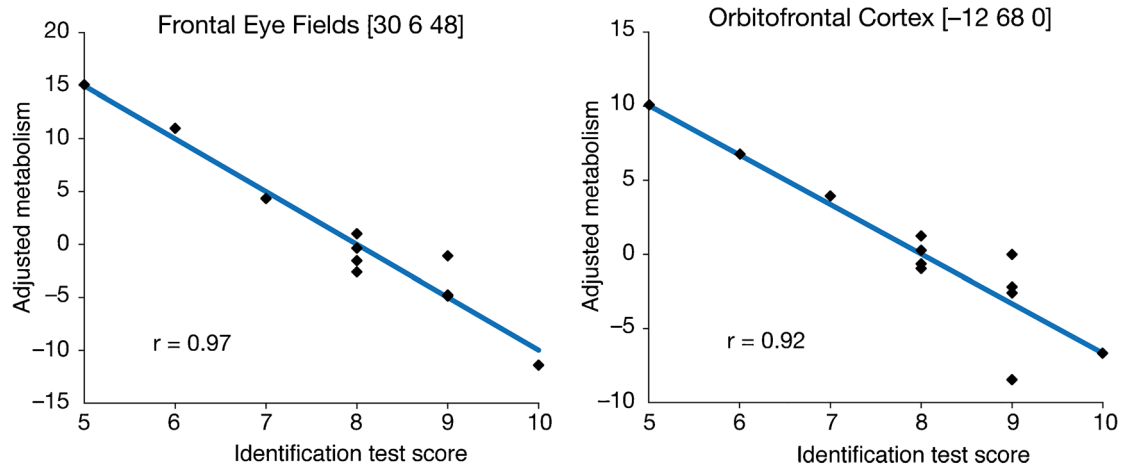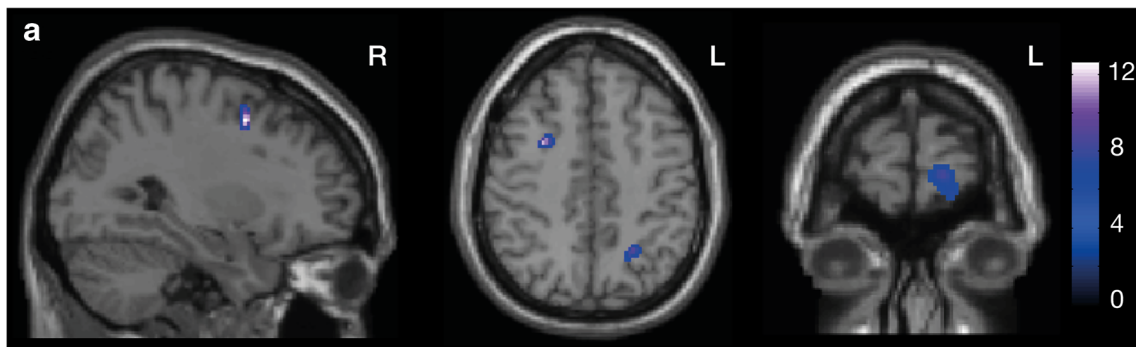
◄ Fig. 4 Results of the correlation analyses performed between the cerebral glucose metabolism and the severity of olfactory dysfunction and between the cerebral glucose metabolism and the duration of anosmia. (**a**) Regression plots of the severity of olfactory dysfunction assessed by *the identification test score* (Top) and adjusted metabolic responses obtained by considering the peak voxel in the right FEF ([30 6 48], Pearson's correlation: $r = 0.97$, $p < .001$) and in the left orbitofrontal cortex ([− 12 68 0], Pearson's correlation: $r = 0.94$, $p < .001$). (**b**) Regression plots of the duration of anosmia (Bottom) and adjusted metabolic responses obtained by considering the peak voxel in the right DLPFC ([38 32 34], Pearson's correlation: $r = 0.94$, $p < .001$) and in the

our laboratory. Further studies should investigate those aspects in large cohorts of patients.

Conclusions

This PET-MR study demonstrates that the main pathophysiological hypotheses (i.e., obliteration of the olfactory cleft, central involvement due to SARS-CoV-2 neuroinvasiveness) raised to explain sudden smell loss in COVID-19 do not explain dysosmia in all patients. It also shows that smell loss is associated with cerebral metabolic changes in core olfactory and other brain areas possibly related to combined processes of deafferentation and active functional reorganization secondary to the lack of olfactive sensory stimulation. Based on those findings, SARS-CoV-2-infection limited to OE support and stem cells might be the predominant pathophysiological mechanisms involved in COVID-19 sudden loss of smell, with variable interindividual structural and functional consequences.

Compliance with ethical standards

Role of the funder/sponsor The funding sources had no role in the design and conduct of the study (collection, management, analysis, and interpretation of data); in the preparation, review, and approval of the manuscript; and decision to submit the manuscript for publication.

Standard protocol approvals, registrations, and patient consents Studies were carried out at the CUB Hôpital Erasme

(Brussels, Belgium). Participants contributed to the corresponding studies approved by the institutional Ethics Committee after written informed consent (References: P2020/204, CCB: B4062020000031; P2017/541, CCB: B406201734197).

References

1. Cooper KW, Brann DH, Farruggia MC, Bhutani S, Pellegrino R, Tsukahara T, et al. COVID-19 and the chemical senses: supporting players take center stage. Neuron. 2020;107:219–33.
2. Hoffmann M, Kleine-Weber H, Schroeder S, Krüger N, Herrler T, Erichsen S, et al. SARS-CoV-2 cell entry depends on ACE2 and TMPRSS2 and is blocked by a clinically proven protease inhibitor. Cell. 2020;181:271–80.e8.
3. Politi LS, Salsano E, Grimaldi M. Magnetic resonance imaging alteration of the brain in a patient with coronavirus disease 2019 (COVID-19) and Anosmia. JAMA Neurol. 2020. https://doi.org/10.1001/jamaneurol.2020.2125.
4. Laurendon T, Radulesco T, Mugnier J, Gérault M, Chagnaud C, El Ahmadi A-A, et al. Bilateral transient olfactory bulbs edema during COVID-19-related anosmia. Neurology. 2020. https://doi.org/10.1212/WNL.0000000000009850.
5. Coolen T, Lolli V, Sadeghi N, Rovaï A, Trotta N, Taccone FS, et al. Early postmortem brain MRI findings in COVID-19 non-survivors. Neurology. 2020. https://doi.org/10.1212/WNL.0000000000010116.
6. Klironomos S, Tzortzakakis A, Kits A, Öhberg C, Kollia E, Ahoromazdae A, et al. Nervous System Involvement in Coronavirus Disease 2019: Results from a Retrospective Consecutive Neuroimaging Cohort. Radiology. 2020;297(3):e324-34.
7. Aragão MFVV, Leal MC, Cartaxo Filho OQ, Fonseca TM, Valença MM. Anosmia in COVID-19 associated with injury to the olfactory bulbs evident on MRI. AJNR Am J Neuroradiol. 2020. https://doi.org/10.3174/ajnr.A6675.
8. Guedj E, Million M, Dudouet P, Tissot-Dupont H, Bregeon F, Cammilleri S, et al. 18F-FDG brain PET hypometabolism in post-SARS-CoV-2 infection: substrate for persistent/delayed disorders? Eur J Nucl Med Mol Imaging. 2020. https://doi.org/10.1007/s00259-020-04973-x.
9. Karimi-Galougahi M, Yousefi-Koma A, Bakhshayeshkaram M, Raad N, Haseli S. FDG PET/CT scan reveals hypoactive orbitofrontal cortex in anosmia of COVID-19. Acad Radiol. 2020;27:1042–3.
10. Lund VJ, Mackay IS. Staging in rhinosinusitus. Rhinology. 1993;31:183–4.
11. Trotta N, Goldman S, Legros B, Ligot N, Guerry N, Baete K, et al. Metabolic evidence for episodic memory plasticity in the nonepileptic temporal lobe of patients with mesial temporal epilepsy. Epilepsia. 2011;52:2003–12.
12. De Tiège X, Goldman S, Laureys S, Verheulpen D, Chiron C, Wetzburger C, et al. Regional cerebral glucose metabolism in epilepsies with continuous spikes and waves during sleep. Neurology. 2004;63:853–7.
13. De Tiège X, Ligot N, Goldman S, Poznanski N, de Saint MA, Van Bogaert P. Metabolic evidence for remote inhibition in epilepsies with continuous spike-waves during sleep. Neuroimage. 2008;40:802–10.
14. Trotta N, Archambaud F, Goldman S, Baete K, Van Laere K, Wens V, et al. Functional integration changes in regional brain glucose metabolism from childhood to adulthood. Hum Brain Mapp. 2016;37:3017–30.
15. Trotta N, Goldman S, Legros B, Baete K, Van Laere K, Van Bogaert P, et al. Changes in functional integration with the non-

epileptic temporal lobe of patients with unilateral mesiotemporal epilepsy. PLoS One. 2013;8:e67053.

16. Savic I. Brain imaging studies of the functional organization of human olfaction. Neuroscientist. 2002;8:204–11.

17. Levy LM, Henkin RI, Hutter A, Lin CS, Martins D, Schellinger D. Functional MRI of human olfaction. J Comput Assist Tomogr. 1997;21:849–56.

18. Zhou G, Lane G, Cooper SL, Kahnt T, Zelano C. Characterizing functional pathways of the human olfactory system. Elife. 2019;8. https://doi.org/10.7554/eLife.47177.

19. Qureshy A, Kawashima R, Imran MB, Sugiura M, Goto R, Okada K, et al. Functional mapping of human brain in olfactory processing: a PET study. J Neurophysiol. 2000;84:1656–66.

20. Micarelli A, Chiaravalloti A, Danieli R, Schillaci O, Alessandrini M. Cerebral metabolic changes related to clinical parameters in idiopathic anosmic patients during olfactory stimulation: a pilot investigation. Eur Arch Otorhinolaryngol. 2017;274:2649–55.

21. Kim YK, Hong S-L, Yoon EJ, Kim SE, Kim J-W. Central presentation of postviral olfactory loss evaluated by positron emission tomography scan: a pilot study. Am J Rhinol Allergy. 2012;26:204–8.

22. Poellinger A, Thomas R, Lio P, Lee A, Makris N, Rosen BR, et al. Activation and habituation in olfaction—an fMRI study. Neuroimage. 2001;13:547–60.

23. Rozin P. "Taste-smell confusions" and the duality of the olfactory sense. Percept Psychophys. 1982;31:397–401.

24. Spence C. Just how much of what we taste derives from the sense of smell? Flavour. 2015;4:1–10.

25. Naeini AS, Karimi-Galougahi M, Raad N, Ghorbani J, Taraghi A, Haseli S, et al. Paranasal sinuses computed tomography findings in anosmia of COVID-19. Am J Otolaryngol. 2020:102636. https://doi.org/10.1016/j.amjoto.2020.102636.

26. Chetrit A, Lechien JR, Ammar A, Chekkoury-Idrissi Y, Distinguin L, Circiu M, et al. Magnetic resonance imaging of COVID-19 anosmic patients reveals abnormalities of the olfactory bulb: preliminary prospective study. J Infect. 2020. https://doi.org/10.1016/j.jinf.2020.07.028.

27. Lechien JR, Michel J, Radulesco T, Chiesa-Estomba CM, Vaira LA, De Riu G, et al. Clinical and radiological evaluations of COVID-19 patients with anosmia: preliminary report. Laryngoscope. 2020. https://doi.org/10.1002/lary.28993.

28. Lechien JR, Chiesa-Estomba CM, Hans S, Barillari MR, Jouffe L, Saussez S. Loss of Smell and taste in 2013 European patients with mild to moderate COVID-19. Ann Intern Med. 2020. https://doi.org/10.7326/m20-2428.

29. Galougahi MK, Ghorbani J, Bakhshayeshkaram M, Naeini AS, Haseli S. Olfactory bulb magnetic resonance imaging in SARS-CoV-2-induced anosmia: the first report. Acad Radiol. 2020;27:892–3.

30. Eliezer M, Hautefort C, Hamel A-L, Verillaud B, Herman P, Houdart E, et al. Sudden and complete olfactory loss of function as a possible symptom of COVID-19. JAMA Otolaryngol Head Neck Surg. 2020:674. https://doi.org/10.1001/jamaoto.2020.0832.

31. Kremer S, Lersy F, Anheim M, Merdji H, Schenck M, Oesterlé H, et al. Neurologic and neuroimaging findings in COVID-19 patients: a retrospective multicenter study. Neurology. 2020. https://doi.org/10.1212/WNL.0000000000010112.

32. Zambreanu L, Lightbody S, Bhandari M, Hoskote C, Kandil H, Houlihan CF, et al. A case of limbic encephalitis associated with asymptomatic COVID-19 infection. J Neurol Neurosurg Psychiatry. 2020. https://doi.org/10.1136/jnnp-2020-323839.

33. Pilotto A, Masciocchi S, Volonghi I, del Zotto E, Magni E, De Giuli V, et al. The clinical spectrum of encephalitis in COVID-19 disease: the ENCOVID multicentre study. Medrxiv. 2020. https://doi.org/10.1101/2020.06.19.20133991.

34. Mori I, Nishiyama Y, Yokochi T, Kimura Y. Olfactory transmission of neurotropic viruses. J Neurovirol. 2005;11:129–37.

35. Li Y, Bai W, Hashikawa T. The neuroinvasive potential of SARS-CoV2 may play a role in the respiratory failure of COVID-19 patients. J Med Virol. 2020:552–5. https://doi.org/10.1002/jmv.25728.

36. Wilson DA, Rennaker RL. Cortical activity evoked by odors. In: Menini A, editor. The Neurobiology of Olfaction. Boca Raton: CRC Press/Taylor & Francis; 2011.

37. Reichert JL, Schöpf V. Olfactory loss and regain: lessons for neuroplasticity. Neuroscientist. 2018;24:22–35.

38. Pellegrino R, Farruggia MC, Small DM, Veldhuizen MG. Beyond olfactory cortex - severity of post-traumatic olfactory loss is associated with response to odors in frontal-parietal-insular networks. Medrxiv. 2020. https://doi.org/10.1101/2020.06.09.20118539.

39. Moon W-J, Park M, Hwang M, Kim JK. Functional MRI as an Objective Measure of olfaction deficit in patients with traumatic anosmia. AJNR Am J Neuroradiol. 2018;39:2320–5.

40. Savic I. Brain imaging studies of the functional organization of human olfaction. Chem Senses. 2005;30(Suppl 1):i222–3.

41. Dietemann S, Noblet V, Imperiale A, Blondet C, Namer IJ. FDG PET findings of the brain in sudden blindness caused by bilateral central retinal artery occlusion revealing giant cell arteritis. Clin Nucl Med. 2015;40:45–6.

42. Yang TH, Oh SY, Kwak K, Lee JM. Homonymous visual field loss without structural lesion on magnetic resonance imaging: documented with positron emission tomography and diffusion tensor imaging. Neuroophthalmology. 2014 [cited 2020 Aug 21];38. Available from: https://pubmed.ncbi.nlm.nih.gov/27928306/.

43. Singh AK, Phillips F, Merabet LB, Sinha P. Why does the cortex reorganize after sensory loss? Trends Cogn Sci. 2018;22:569–82.

44. Rinck F, Rouby C, Bensafi M. Which format for odor images? Chem Senses Oxford Academic. 2008;34:11–3.

45. Van Toller S. Assessing the impact of anosmia: review of a questionnaire's findings. Chem Senses. Oxford Academic. 1999;24:705–12.

46. Hu Y, Xu Q, Li K, Zhu H, Qi R, Zhang Z, et al. Gender differences of brain glucose metabolic networks revealed by FDG-PET: evidence from a large cohort of 400 young adults. PLoS ONE. 2013: e83821. https://doi.org/10.1371/journal.pone.0083821.

47. Kawachi T, Ishii K, Sakamoto S, Matsui M, Mori T, Sasaki M. Gender differences in cerebral glucose metabolism: a PET study. J Neurol Sci. 2002;199(1–2):79–83. https://doi.org/10.1016/s0022-510x(02)00112-0.

48. Yoshizawa H, Gazes Y, Stern Y, Miyata Y, Uchiyama S. Characterizing the normative profile of 18F-FDG PET brain imaging: sex difference, aging effect, and cognitive reserve. Psychiatry Res. 2014;221:78–85.